

ORIGINAL ARTICLE

# Laser Cutting as a Rapid Method for Fabricating Thin Soft Pneumatic Actuators and Robots

Amir Ali Amiri Moghadam,<sup>1,2</sup> Seyedhamidreza Alaie,<sup>1,2</sup> Suborna Deb Nath,<sup>1</sup> Mahdie Aghasizade Shaarbaft,<sup>1</sup> James K. Min,<sup>1,2</sup> Simon Dunham,<sup>1,2</sup> and Bobak Mosadegh<sup>1,2</sup>

## Abstract

Pneumatically actuated soft robots address many challenges with interfacing with delicate objects, but these actuators/robots are still bulky and require many hours to fabricate, limiting their widespread use. This article reports a novel design and manufacturing method for ultrathin soft robots and actuators ( $\sim 70 \mu\text{m}$ ) using a laser-cutting machine that cuts/welds sheets of thermoplastic polyurethane (TPU) from a 2D CAD drawing. Using this method, five different soft actuators (e.g., bending, rotating, contracting) are designed, fabricated, and characterized with both planar and nonplanar motions. Furthermore, we show how stacking multiple sheets of TPU enables rapid fabrication of multifunctional actuators. Finally, a portable four-arm swimming robot is designed and fabricated without any assembly steps. This rapid fabrication method enables soft robots to go from concept to operational within minutes, and creates a new subclass of soft robots suitable for applications requiring a robot to be ultrathin, lightweight, and/or fit within small volumes.

**Keywords:** soft robotics, thin pneumatic actuators, thermoplastic polyurethane, laser cutter, rapid fabrication

## Introduction

SOFT ROBOTICS IS an emerging field with great potential for interfacing with delicate objects.<sup>1,2</sup> Soft actuators are made of soft and compliant materials such as polymer/metal composites,<sup>3–5</sup> elastomers,<sup>6,7</sup> and hydrogels.<sup>8,9</sup> These soft machines operate based on pneumatic,<sup>7,10,11</sup> electrical,<sup>3,12,13</sup> chemical,<sup>14,15</sup> and optical<sup>16</sup> actuation mechanisms. Of these, soft pneumatic actuators are particularly interesting due to their low cost, simple operation, and relatively long lifetimes.<sup>7,17,18</sup>

Generally, soft pneumatic actuators comprise a series of interconnected inflatable chambers, which are made from elastomers, fabrics, or a combination of both types of these materials. The geometry and material properties of these chambers dictate the motion of the pneumatic actuators, on actuation. Fabrication of these actuators is usually achieved by rapid casting with two-part mixtures of liquid elastomer precursors into three-dimensional (3D)-printed molds with or without manually embedded fabrics. Although this process is relatively simple compared with other manufacturing methods for soft and hard robotic actuators, the full process of creating a new design for an actuator can take several hours,

since it requires the following steps: (1) design geometry in a 3D CAD, (2) 3D print mold, (3) prepare and degas elastomer, (4) cast and bake elastomer (with or without fabric layers), and (5) de-mold and bond parts of an actuator. Furthermore, fabricating thin ( $<0.5 \text{ mm}$ ) actuators is particularly challenging since currently typical 3D-printed parts do not provide sufficient resolution, and de-molding such thin features can be difficult. In fact, producing small-scale soft actuators requires the use of more specialized design and fabrication methods.<sup>19</sup>

Thin soft actuators can be fabricated by means of soft lithographic techniques,<sup>20–22</sup> photolithography,<sup>23</sup> and microcasting.<sup>24</sup> Alternatively, Ikeuchi and Ikuta have fabricated thin actuators using membrane microembossing by excimer laser ablation (MeME-X).<sup>25</sup> These methods, although effective, are laborious and time-consuming, limiting their adoption to a broader community. Paek *et al.* have proposed a simple fabrication method for the development of small-scale soft actuators, based on dip-coating of cylindrical templates.<sup>19</sup> A drawback to the simplicity of this method, however, is that only a limited number of designs can be fabricated easily. Above-mentioned methods focused on design and fabrication

<sup>1</sup>Dalio Institute of Cardiovascular Imaging, New York-Presbyterian Hospital and Weill Cornell Medicine, New York, New York.

<sup>2</sup>Department of Radiology, Weill Cornell Medicine, New York, New York.

of 3D small-scale actuators. Alternatively, planar designs can be utilized to develop more compact and smaller actuators.

Peano muscles could be considered among the first designs for development of more compact actuators.<sup>26,27</sup> Veale *et al.* have fabricated and modeled linear Peano actuators made of plastic, reinforced plastic, and textile/silicone composites.<sup>27</sup> Park *et al.* proposed the idea of flat pneumatic artificial muscles.<sup>28</sup> These planar air chamber actuators were fabricated in silicone rubber, using a two-stage molding process, while the chambers were fabricated by the application of a release spray over a mask.<sup>28,29</sup> Another set of works by Niiyama *et al.* has introduced pouch motors, which are made of sheets of plastic films fabricated by heat stamping and heat drawing systems.<sup>30,31</sup> They demonstrated that both linear and rotary motions can be achieved using pouch motors. Subsequently, Chang *et al.* have optimized the size of a linear pouch motor for gait rehabilitation.<sup>32</sup> Motivated by the concept of a planar actuator, Yap *et al.* developed actuators made from layers of fabric embedded in a latex balloon.<sup>33</sup> Sung and Rus have demonstrated how robot joints can be fabricated using the print-and-fold process.<sup>34</sup> The 2D design of foldable joints and robots can provide a framework for design of soft planar actuators.

Although the two-dimensional (2D) design of the Peano actuators or pouch motors makes them very compact and thin in their relaxed state, their zero-volume chambers expand to a relatively large volume, on inflation, due to the designs having a large surface area. This large inflation could potentially limit the application of these actuators in situations requiring operation in small spaces such as transcatheter therapies or search and rescue missions. One approach to address this issue is to design 2D actuators that can actuate with relatively small strains and moderate rotations.

In this article, we explore the 2D pattern of soft actuators that can operate under this actuation mechanism. In addition, we

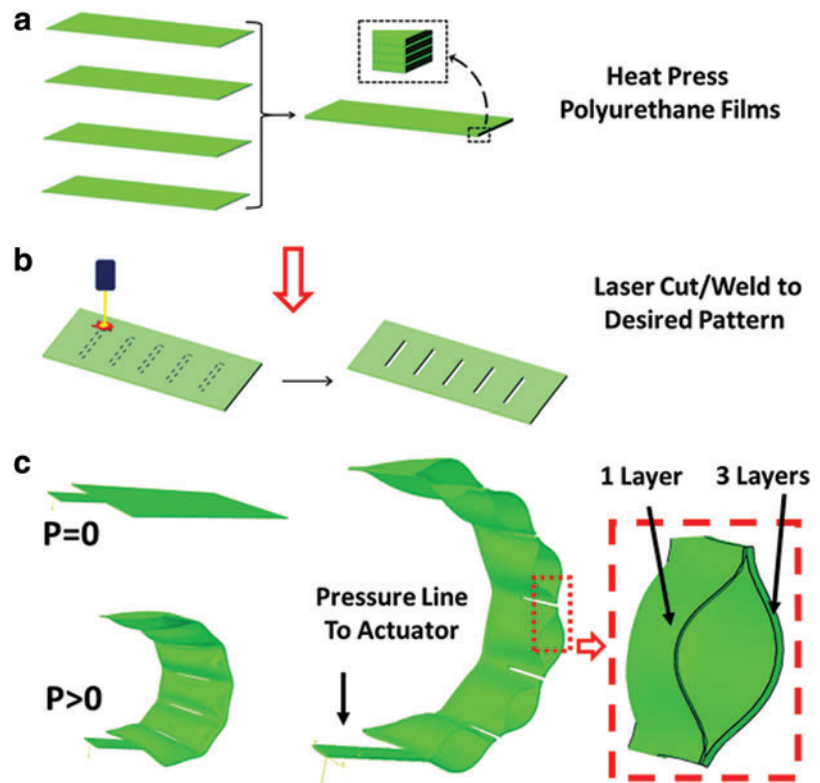
present a simple and effective method for rapid fabrication of thin soft actuators by simultaneously cutting and laser welding<sup>35</sup> a stack of thin films made of thermoplastic polyurethane (TPU, Supplementary Table S1; Supplementary Data are available online at [www.liebertpub.com/soro](http://www.liebertpub.com/soro)). This approach uses inexpensive and commercially available materials and tools for creating these thin actuators (as thin as  $70\ \mu\text{m}$ ) and soft robots. Both the manufacturing method and design of the proposed actuators in the current work are different from those of pouch motors.<sup>30,31</sup> Pouch motors have two main layers, namely the actuator and structure layer. The actuator layer is a thermoplastic film, whereas the structure layer, which acts as a scaffold of the actuator, is made of a stiff material (e.g., plastics).<sup>30,31</sup> The actuator layer is fabricated by means of heat stamping and heat drawing systems. These methods only bond the thermoplastic films and cannot cut the actuator pattern. Thus, the fabrication method requires a cutting step by means of laser cutter or cutting plotter. Moreover, there is an assembly step to bond/glue the actuator layer to the structure layer. In contrast, the proposed actuator in the current work is made of one material (thermoplastic film), and both cutting and welding of the films comprising the actuator occur in one step, using a laser cutter (Supplementary Table S2).

Using this method, we propose several different types of thin actuators, whose various motions occur in-plane and out-of-plane. The trajectory of these actuators is modeled using the finite element method (FEM), which is in agreement with acquired experimental data. Furthermore, we demonstrate the use of thin soft grippers for pick-and-place applications and a swimming soft robot.

## Methods

Actuators were made from commercially available TPU films with a thickness of  $\sim 37\ \mu\text{m}$  (Stretchlon<sup>®</sup> 200 High

**FIG. 1.** Fabrication process. (a) Four layers of thermoplastic polyurethane are heat pressed to conformal contact. (b) A laser beam cuts the layers with a desired pattern. (c) The inflated chamber is bounded by one and three layers on its sides; the asymmetry of the stiffness leads to a bending motion. Color images available online at [www.liebertpub.com/soro](http://www.liebertpub.com/soro)



Stretch Bag Film) and a heat press (Power Heat Press QX-A1) and a laser cutter (Universal Laser System VLS2.3), as illustrated in Figure 1. Four layers of polyurethane film were heat pressed for 2 min at the temperature of  $\sim 77^{\circ}\text{C}$ . The pressure knob was manually adjusted such that the films did not form a permanent bond. The multilayer film was cut/welded into the desired pattern using a laser cutter (100% speed, 500 pulses per inch, and 80% power). The actuators were inflated using a precise fluid dispenser (Nordson EFT, Ultimius I) and the actuator motion was recorded by a Canon 5DMark III full frame camera fitted with a 100 mm/f2.8 IS macro lens. The actuation pressure was measured using a 015D44R Honeywell pressure sensor. FEM (using ABAQUS software) was used to simulate the deformation of the soft actuators using 3D shell elements and a hyperelastic material model. Considering the symmetrical shape of the actuators, only half of the actuators were modeled using symmetrical boundary conditions. An ABB robotic arm (6 DOF ABB, IRB120) was used to demonstrate the pick-and-place tasks (Supplementary Data; Supplementary Data are available online at [www.liebertpub.com/soro](http://www.liebertpub.com/soro)).

The soft gripper was controlled using four solenoid valves (VQ110U-5M). To synchronize the operation of the soft gripper with that of the robot, we used four digital outputs of the robot control system to actuate the gripper, and ABB RAPID programming language was utilized to control both the robot and its soft gripper.

**Results**

*Fabrication of soft thin actuators using a laser cutter*

The method for producing thin actuators started with heat pressing films of TPU to ensure they were flat and in conformal contact without creating a permanent bond between the layers (Fig. 1a). Next, a laser cutting machine was used to create the desired shape of the actuator. Conveniently, the sheets of the polyurethane are welded by the laser cutting machine. A single pass of the laser beam, therefore, both cut

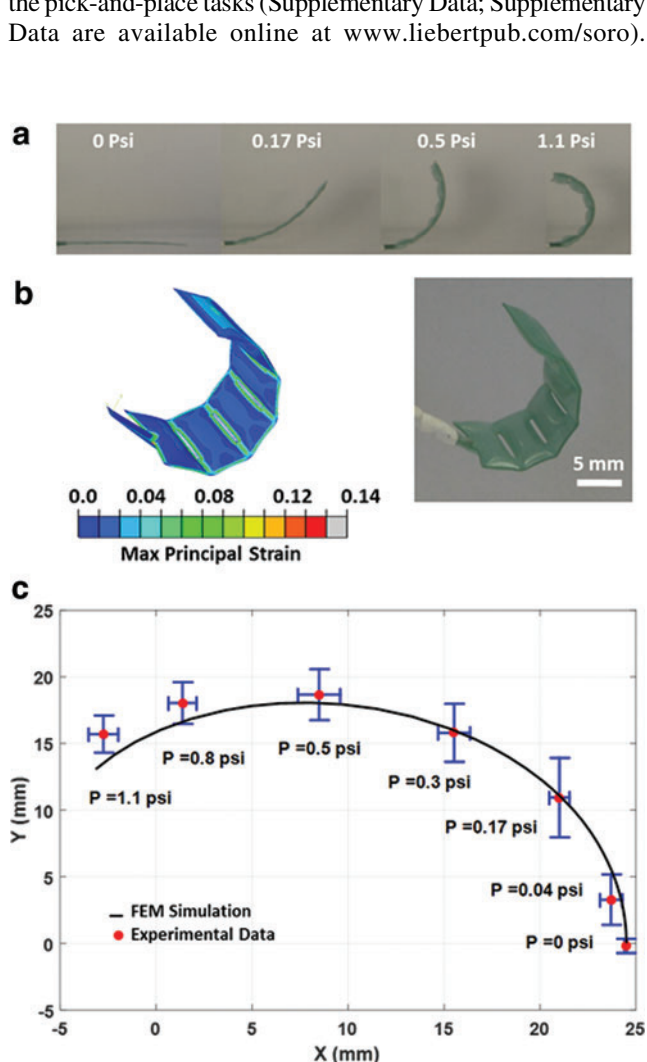


**FIG. 2.** Bending actuator type I. (a) Sequence of images showing the bending motion of actuator type I. (b) Comparing the ultimate bending configuration of the actuator with that of FEM simulation. (c) Comparison between the simulated and experimental lateral displacements of the thin ACTUATOR. FEM, finite element method. Color images available online at [www.liebertpub.com/soro](http://www.liebertpub.com/soro)

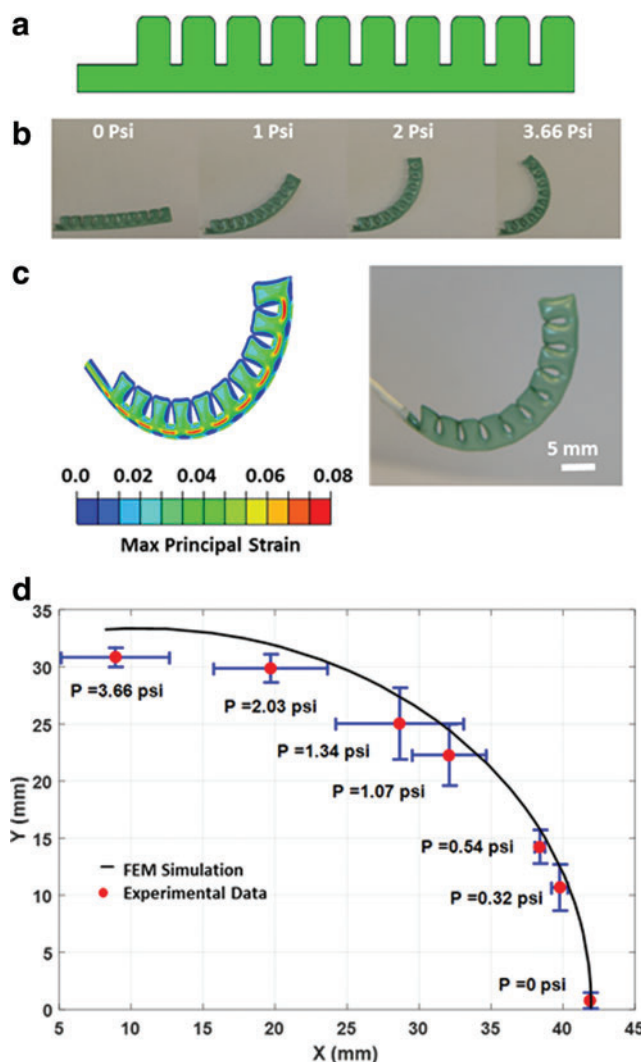


**FIG. 3.** Bending actuator type II. (a) Asymmetric 2D profile for actuator type II. (b) Sequence of images showing the bending motion of actuator type II. (c) Comparing the ultimate bending configuration of the actuator with that of FEM simulation. (d) Comparison between simulated and experimental lateral displacements of the thin ACTUATOR. Color images available online at [www.liebertpub.com/soro](http://www.liebertpub.com/soro)

and bonded the edges of the actuator, forming a sealed thin actuator, which was functional immediately after the cutting process (Fig. 1b). Variation of the parameters for the lamination step (i.e., heat press temperature, pressure, and time) and the laser cutting step (i.e., speed, power, and pulse per inch) affects the performance of the thin actuator. We, therefore, characterized these parameters to yield two-layered actuators that, on average, can hold  $\sim 10$  psi for a square ( $20 \times 20$  mm) geometry (Supplementary Note S1 and Supplementary Fig. S1). The tensile test data of TPU film is shown in Supplementary Figure S2 and Supplementary Table S3.

One conventional method to produce a bending actuator is to create an asymmetrical profile, which can be achieved by making one side of the actuator thicker or less compliant than the other side.<sup>21</sup> As a result, an actuator bends on inflation due to the asymmetric stiffness and strain on its sides (Supplementary Note S2). Figure 1 demonstrates this principle using a four-layer actuator (actuator type I), with in-plane symmetry (Supplementary Video S1 and Supplementary Fig. S3). The inflated actuator was bounded by single- and triple-layered films (Fig. 1c), which led to the asymmetry across the actuator. All four layers were laminated together and subsequently laser cut/welded at the same time. While the actuator can work with one thicker layer as well, using the four-layer fabrication method has the advantage that the actuator is able to actuate bidirectionally. The motion of this actuator is shown in Figure 2a, and the actuation mechanism was further elucidated by simulations. Supplementary Fig. S4 demonstrates the effect of geometrical parameters on the bending displacement of actuator type I. Alternatively, the aforementioned asymmetrical profile could be achieved directly by the geometry of the actuator. Figure 3a depicts such a geometry that comprised several pockets connected only on one side (actuator type II).

It must be noted that actuator type II is symmetrical through its thickness and thus has two layers of TPU on each side. Supplementary Note S3, discusses the effect of pressure and size on the blocking force of this actuator. In contrast to actuator type I, the motion of this actuator occurred in-plane (Fig. 3b and Supplementary Video S2).

The motions for both these types of actuators with in- and out-of-plane bending were simulated using FEM (Supplementary Note S4 and Supplementary Fig. S2); the simulation agreed with the experimental data (Figs. 2b, c and 3c, d). The FEM model showed that the level of strain for both actuators was relatively low ( $<15\%$ ), compared with conventional soft pneumatic actuators, which typically require ( $>50\%$ ). These simulations also visualized the distribution of strain, showing that the majority of the actuator was undergoing even lower levels of strain ( $<5\%$ ). These low levels of strain suggest that the mechanism of bending for these actuators was primarily dependent on folding of the walls of the chambers. This behavior is different than most soft pneumatic actuators, which rely on large ( $>50\%$ ) levels of strain of the chamber walls.<sup>7</sup> In comparing the designs of these two types of actuators, actuator type II (Fig. 3c) had a lower and more uniform strain distribution for nearly the same degree of bending. The bending displacement of these actuators under different pressure inputs is shown in Supplementary Figures S3 and S5. The soft actuators can be considered nonlinear springs, where the stiffer the actuator the more force it can generate. Supplementary Figures S3, S5, and S8 simulate the deformation of the actuators versus the input pressure, and have the potential to provide insight into the stiffness and generated force of the actuators, in future analysis. Supplementary Figure S6 shows the blocking force of bending actuator type II under different pressure inputs and sizes.

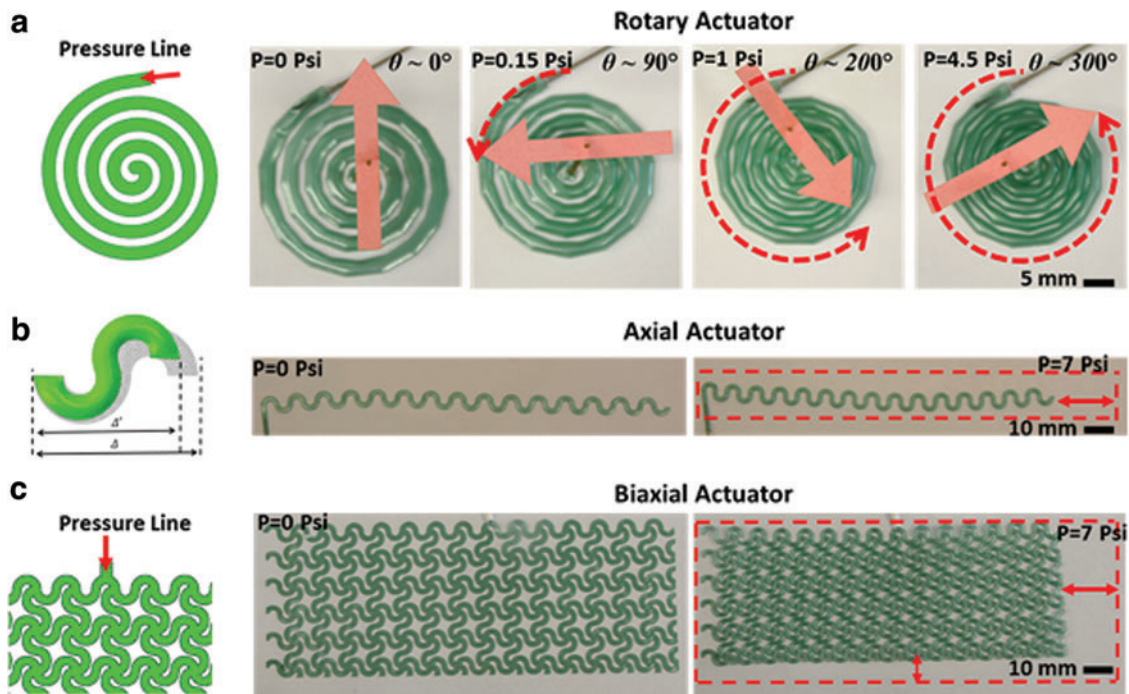


**FIG. 4.** Other types of actuators. (a) Schematic and prototype of a rotary actuator ( $300^\circ$  rotation). (b) Schematic unit cell and prototype of an axial actuator (unactuated and actuated states). (c) Schematic and prototype of a biaxial actuator (unactuated and actuated states). Color images available online at [www.liebertpub.com/soro](http://www.liebertpub.com/soro)

### Alternate designs for thin soft actuators

So far, we have detailed the design and fabrication of in-plane and out-of-plane bending actuators. However, the design of functional soft robots/machines with complex motions requires other types of actuators, such as rotary and linear actuators (Supplementary Figs. S7–S9). Using the method described above, these types of actuators can be simply fabricated just by changing the design of the 2D CAD file used to laser cut the actuators.

The design of a rotary actuator was motivated by the working principle of the Bourdon tube, which generally consists of a curved tube with a flattened cross-sectional area.<sup>36</sup> Typically, Bourdon tubes have a rectangular cross section where the longer side is parallel to the normal of the plain of the curved tube. On inflation, the cross section tends toward a nearly round shape causing the tube to straighten and extend.<sup>36</sup> The relationship between the tip displacement and the internal pressure is commonly used to measure the pressure of a system.<sup>36</sup> However, recently, Bourdon designs have been utilized for hydraulic actuators for microelectromechanical systems (MEMS),<sup>36</sup> and soft

surgical robots.<sup>36,37</sup> Leveraging this design principle, we used the laser cutter to fabricate a soft thin rotary actuator with circular and spiral curves. The cross section of a conventional Bourdon tube is longer out-of-plane than in-plane, whereas our actuators were longer in-plane (Supplementary Fig. S7). Consequently, on inflation, the thin rotary actuator that we fabricated curled, whereas the conventional Bourdon tube straightens (Supplementary Note S5). Figure 4a demonstrates how a spiral curve acts as a rotary actuator (Supplementary Video S3). On inflation, the actuator could rotate up to 300° at a pressure of ~31.03 kPa (4.5 psi).

Axial and biaxial actuators were fabricated by laser cutting lattice-type patterns with unit cells that incorporated these types of curved features. Axial actuators were developed from a linear array of semicircle curves, with an S-shaped unit cell (Fig. 4b). This unit cell is known as a horseshoe serpentine lattice, which has been used for many applications, such as stretchable electronics.<sup>38,39</sup> On inflation, each semicircular curve curled, thus decreasing the overall length of an S-shaped unit cell (Supplementary Video S4). Changing the shape and total number of unit cells allowed us to modify the overall

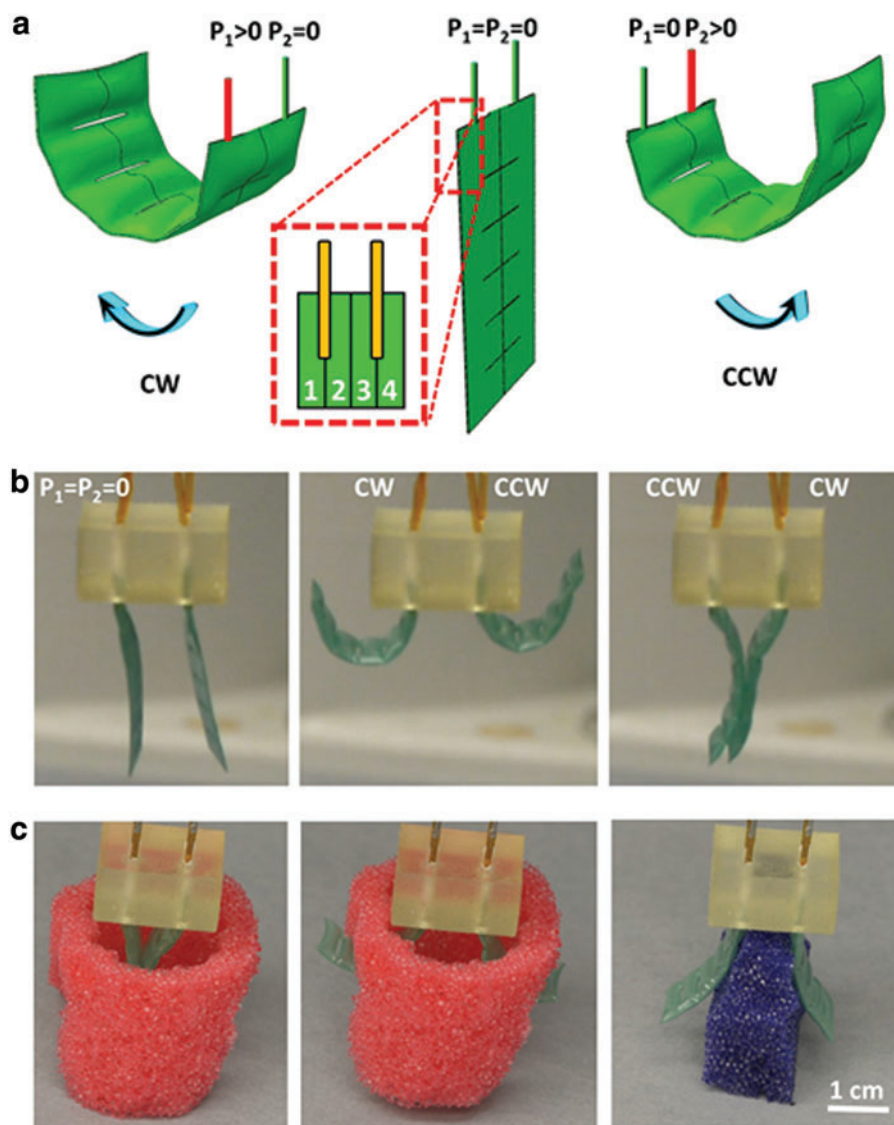


**FIG. 5.** Development of a soft gripper. **(a)** Schematic of a bidirectional soft actuator and design of its working principle. **(b)** Images of the unactuated, open, and close configurations for this thin ACTUATOR. **(c)** Images depicting how these different configurations grasp objects for the pick-and-place task. CW, clockwise; CCW, counterclockwise. Color images available online at [www.liebertpub.com/soro](http://www.liebertpub.com/soro)

displacement of the linear actuator. For instance, a linear actuator with 15 U cells generated approximately a 20 mm displacement at a pressure of  $\sim 48.2$  kPa (7 psi), suggesting each unit cell displaced  $\sim 1.3$  mm (Fig. 4b). The developed axial actuator was extended to a biaxial actuator (Fig. 4c) creating a 2D serpentine pattern. A unit cell for a biaxial actuator was made by rotating the S-shaped unit cell by  $90^\circ$  and joining it to itself (Supplementary Video S5). The overall displacement of each axis was linearly proportional to the number of S-shaped unit cells used in that direction. For example, the biaxial actuator in Figure 4c, which has 15 and 6 U cells along the  $x$  and  $y$  directions, respectively, contracted about 20 and 7.4 mm at a pressure of  $\sim 48.2$  kPa (7 psi).

To further demonstrate the versatility of thin actuators, we showed that actuator type I can function as a bidirectional actuator simply by inflating between its different layers. Specifically, inflating the chamber bounded by layers 1 and 2 resulted in a clockwise motion, and inflating the chamber bounded by layers 3 and 4 resulted in a counterclockwise motion (Fig. 5a). By combining two of these bidirectional actuators with a robotic arm, we created a soft gripper capable of performing pick-and-place tasks (Supplementary Note S6, Supplementary Videos S6, S7, and Supplementary Fig. S10). Figure 5b and c shows the unactuated, open, and close configurations of the gripper, as well as the images taken during the pick-and-place operations for different objects. In its open configuration, at a pressure of  $\sim 41$  kPa (6 psi), the gripper successfully lifted an object (2.66 g), which was 30 times heavier than its own weight (0.098 g).

#### Swimming robot

As a final demonstration of this fabrication method, we designed and fabricated a four-arm swimming robot. The 2D CAD file of the robot was directly fabricated into a robotic swimmer in one step without requiring any assembly. Each arm had two degrees of freedom (DOFs) and consisted of two bending actuators. The first actuator (actuator type II with in-plane bending motion) acted as the arm of the swimmer, and the second actuator (actuator type I with out-of-plane bending motion) acted as the fin (Fig. 6a). The palm of this robot was a circular balloon that connects the fin to its arm. When actuated, the palm inflated more than the rest of the arm, due to its large and circular surface area, allowing it to serve as the point of contact of the robot to the water and ensuring the arm stays level with the surface of the water during actuation. Because of its light weight (0.62 g) and large surface area, the robot floated in both its actuated and unactuated states.

The robot was powered by a portable actuation system that included a battery, minicompressor, microcontroller, and a three-way valve (Supplementary Fig. S11 and Supplementary Note S7). To demonstrate that the swimming motion is not due to the momentum of the exhausted air, we designed two versions of the robot. Supplementary Figure S12 shows a schematic of the same swimming robot in Figure 6a, but with actuators that are mirrored so the robot swims in the opposite direction; the mirrored robot swam in the opposite direction, confirming the hypothesis (Supplementary Video S8). Figure 6b and c shows the unactuated and actuated configurations of the forward swimming robot (Supplementary

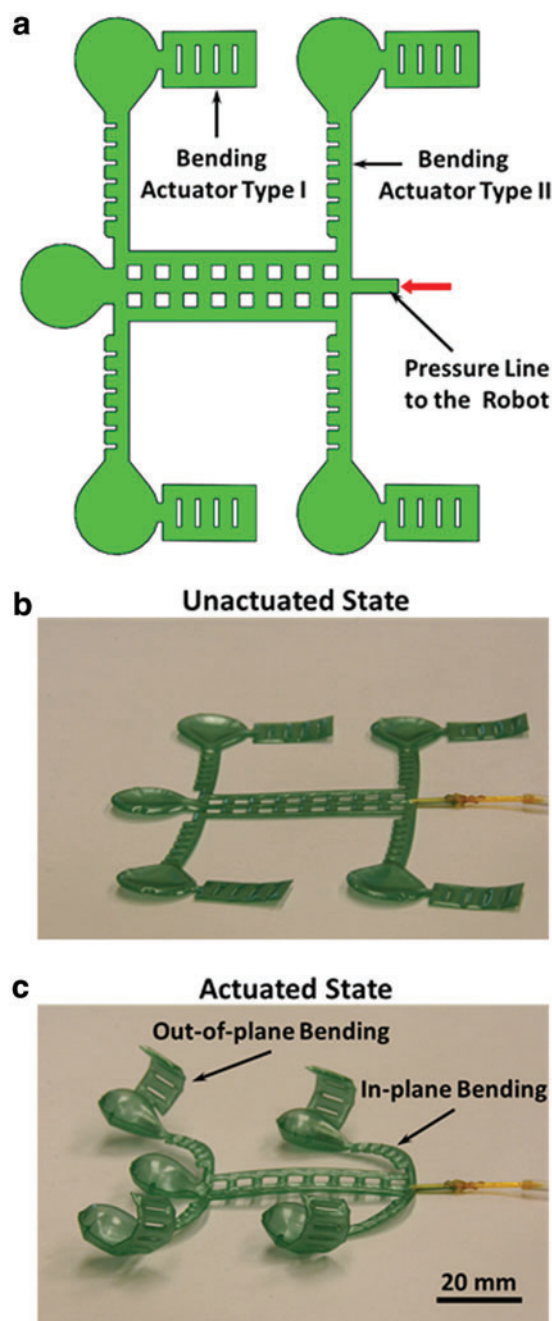


**FIG. 6.** Development of a swimming robot. (a) Schematic design of swimming robot for generating forward swimming motions. (b, c) Unactuated and actuated configurations in forward motion mode. Color images available online at [www.liebertpub.com/soro](http://www.liebertpub.com/soro)

Video S9); it should be noted that the robot is upside down (i.e., laying on its back) to better visualize the motion of the actuators.

Figure 7a shows a sequence of images of the forward swimming motion for a single cycle, where a cycle consists of an inflation and deflation phase. Since the flow rate of the compressor was relatively low ( $<250$  mL/min), the arms of the robot bent gradually and therefore produced little thrust. During the deflation phase, however, the arms returned to their original position more quickly, creating a relatively

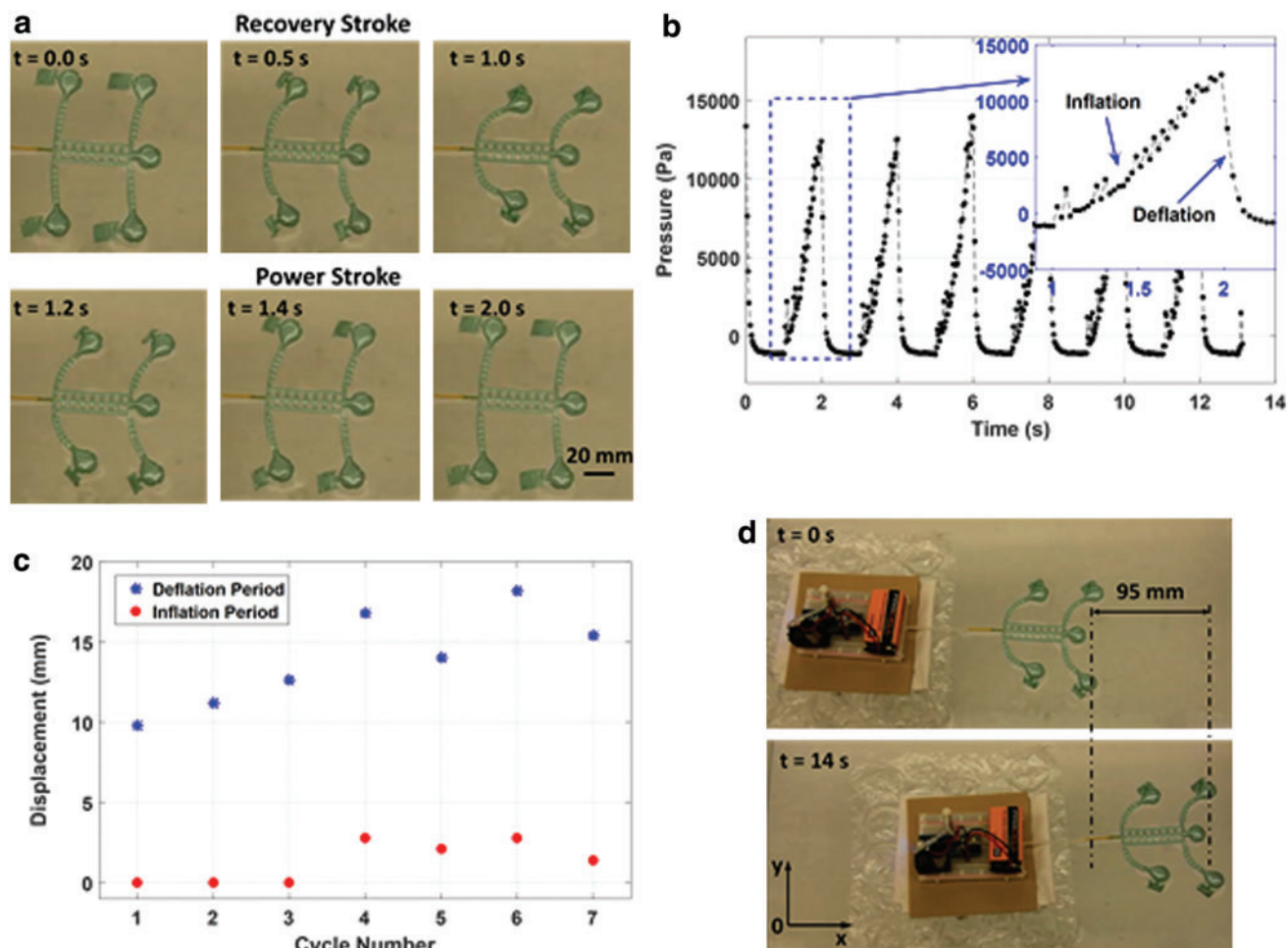


**FIG. 7.** Analysis of swimming motion. (a) Sequence of swimming motion for one cycle. (b) Pressure inside the robot during the inflation and deflation periods. (c) Horizontal displacement of robot during the inflation and deflation phases. (d) Total displacement after seven cycles (14 s). Color images available online at [www.liebertpub.com/soro](http://www.liebertpub.com/soro)

greater thrust than during the inflation phase. Therefore, the inflation phase served as the recovery stroke, and the deflation phase served as the power stroke for this swimming robot. Figure 7b shows the pressure inside the robot during the inflation and deflation phases. The graph shows that the inflation occurred in a near-linear manner over 1 s, while the deflation occurred exponentially, dropping 95% of its pressure in  $\sim 500$  ms. Figure 7c shows the displacement of the robot for the deflation and inflation phases over a series of seven cycles. Initially during the first three cycles, the robot had a near-zero movement during its inflation phase and a progressively increasing displacement during its deflation phase. After the initial three cycles, the inflation phase has a baseline displacement of  $\sim 14$  mm. Over the seven cycles, the average velocity of the robot was 6.7 mm/s (Fig. 7d), starting from 5 mm/s and increasing to 8.4 mm/s during the seventh cycle. The soft robot was able to pull a load of 127 g, 204 times its own weight.

## Discussion

The described method for fabrication of thin actuators has several advantages over conventional fabrication methods: (1) *Simple design of geometries.* Conventional methods

require designs to be made in 3D CAD and then translated into molds for 3D printing. Thin actuators only require a 2D layout and can be directly cut onto thermoplastic films. (2) *Arbitrary 2D geometries.* Since the laser cutter can be programmed to cut almost any geometry, thin actuators of various sizes and shapes can be rapidly tested for discovering novel motions. (3) *Rapid Fabrication.* The bonding between the thermoplastic films occurs immediately in the proposed method. Therefore, fabrication of novel thin actuators can be done within minutes, compared with several hours with conventional methods. (4) *Versatile thickness.* Since the process utilizes prefabricated films that can be obtained with high quality and uniformity, therefore, one can fabricate planar actuators with a thickness much smaller than what can be achieved by 3D molding. (5) *Composite material integration.* Materials with different properties can easily be directly laminated to achieve desired motions or properties. (6) *Scalability.* An array of thin actuators can be made from a single sheet of laminated films, and is only limited by the area of the laser cutter and heat press. This article demonstrates several designs for effective actuators, but we have found that designs that are symmetric in both thickness and geometry tend to yield ineffective movement (i.e., simple expansion), and that materials with elastic properties are needed to

actuate repeatedly. Moreover, the proposed fabrication method is limited to cutting/welding thin sheets of thermoplastics and therefore limited in the types of materials able to be utilized. In addition, since this method cuts planar sheets, direct fabrication of 3D actuators is not possible, but manual assembly of planar actuators into a 3D robot should be feasible.

Soft pneumatic actuators are particularly useful in applications that require the actuators to be lightweight and/or fit within small volumes. We envision such applications to be transcatheter surgical grippers, wearable actuators, and untethered battery-powered mobile (e.g., walking, flying, and swimming) robots. Currently, the major limitation with thin actuators is that their overall force is low. This limitation of force can be improved by use of superior composite materials with higher young's modulus, toughness, and strength, such that higher pressures can be applied. This work provides a framework for future studies on other geometric designs to produce different types of motions and to optimize the actuation lifetimes and efficiency.

### Acknowledgments

We thank the Dalio Institute of Cardiovascular Imaging for its support. Research reported in this publication was supported by the National Center for Advancing Translational Sciences of the National Institutes of Health under Award Number UL1TR000457.

### Authors' Contributions

A.A.A.M. and B.M. designed the experiments and wrote the article. A.A.A.M. and S.A. developed the laser cutting procedure. A.A.A.M. devised the rotary actuator, bending actuators, and swimming robot. A.A.A.M. and S.A. devised the axial and biaxial actuators. S.N. characterized the laser cutting parameters. A.A.A.M. and M.S. performed the pick-and-place experiment. J.M., S.A., and S.D. edited the article. J.M. oversaw this research.

### Supporting Information

Supporting information is available from the Online Library or from the author.

### Author Disclosure Statement

No competing financial interests exist.

### References

1. Laschi C, Cianchetti M. Soft robotics: new perspectives for robot bodyware and control. *Front Bioeng Biotechnol* 2014;2:3.
2. Rus D, Tolley MT. Design, fabrication and control of soft robots. *Nature* 2015;521:467–475.
3. Shahinpoor M, Kim KJ. Ionic polymer-metal composites: I. Fundamentals. *Smart Mater Struct* 2001;10:819–833.
4. Amiri Moghadam AA, *et al.* Nonlinear dynamic modeling of ionic polymer conductive network composite actuators using rigid finite element method. *Sens Actuat A Phys* 2014;217:168–182.
5. Amiri Moghadam AA, Alizadeh V, Tahani M, Kouzani A, Kaynak A. Equivalent dynamic thermoviscoelastic modeling of ionic polymers. *Polym Adv Technol* 2015;26:385–391.
6. Ilievski F, Mazzeo AD, Shepherd RF, Chen X, Whitesides GM. Soft Robotics for Chemists. *Angew Chem Int Ed* 2011;50:1890–1895.
7. Mosadegh B, *et al.* Pneumatic networks for soft robotics that actuate rapidly. *Adv Funct Mater* 2014;24:2163–2170.
8. Ionov L. Hydrogel-based actuators: possibilities and limitations. *Mater Today* 2014;17:494–503.
9. Banerjee H, Ren H. Optimizing double-network hydrogel for biomedical soft robots. *Soft Robot* 2017. DOI:10.1089/soro.2016.0059.
10. Yang D, *et al.* Buckling of elastomeric beams enables actuation of soft machines. *Adv Mater* 2015;27:6323–6327.
11. Agarwal G, Besuchet N, Audergon B, Paik J. Stretchable materials for robust soft actuators toward assistive wearable devices. *Sci Rep* 2016;6:34224.
12. Moghadam AAA, Kouzani A, Torabi K, Kaynak A, Shahinpoor M. Development of a novel soft parallel robot equipped with polymeric artificial muscles. *Smart Mater Struct* 2015;24:35017.
13. Amiri Moghadam AA, *et al.* Control-oriented modeling of a polymeric soft robot. *Soft Robot* 2016;3:82–97.
14. Wehner M, *et al.* An integrated design and fabrication strategy for entirely soft, autonomous robots. *Nature* 2016; 536:451–455.
15. Zhao Q, *et al.* An instant multi-responsive porous polymer actuator driven by solvent molecule sorption. *Nat Commun* 2014;5:ncomms5293.
16. Wie JJ, Shankar MR, White TJ. Photomotility of polymers. *Nat Commun* 2016;7:13260.
17. Wood RJ, Walsh C. Smaller, softer, safer, smarter robots. *Sci Transl Med* 2014;5:210–219.
18. Nemiroski A, *et al.* ArthroBots. *Soft Robot* 2017. DOI: 10.1089/soro.2016.0043.
19. Paek J, Cho I, Kim J. Microbotic tentacles with spiral bending capability based on shape-engineered elastomeric microtubes. *Sci Rep* 2015;5:10768.
20. Flexible pneumatic twisting actuators and their application to tilting micromirrors. *Sens Actuat A Phys* 2014;216:426–431.
21. Jeong OC, Konishi S. All PDMS pneumatic microfinger with bidirectional motion and its application. *J Microelectromech Syst* 2006;15:896–903.
22. Konishi S, Shimomura S, Tajima S, Tabata Y. Implementation of soft microfingers for a hMSC aggregate manipulation system. *Microsyst Nanoeng* 2016;2:15048.
23. Lu Y-W, Kim C-J. Microhand for biological applications. *Appl Phys Lett* 2006;89:164101.
24. Gorissen B, De Volder M, De Greef A, Reynaerts D. Theoretical and experimental analysis of pneumatic balloon microactuators. *Sens Actuat A Phys* 2011;168:58–65.
25. Ikeuchi M, Ikuta K. Development of pressure-driven micro active catheter using membrane micro emboss following excimer laser ablation (MeME-X) process. In: 2009 IEEE International Conference on Robotics and Automation. IEEE, 2009, pp. 4469–4472. DOI:10.1109/ROBOT.2009.5152869.
26. Sanan S, Lynn PS, Griffith ST. Pneumatic torsional actuators for inflatable robots. *J Mech Robot* 2014;6:31003.
27. Veale AJ, Xie SQ, Anderson IA. Modeling the Peano fluidic muscle and the effects of its material properties on its static and dynamic behavior. *Smart Mater Struct* 2016;25: 65014.
28. Park Y-L, Santos J, Galloway KG, Goldfield EC, Wood RJ. A soft wearable robotic device for active knee motions

- using flat pneumatic artificial muscles. In: 2014 IEEE International Conference on Robotics and Automation (ICRA). IEEE, 2014, pp. 4805–4810. DOI:10.1109/ICRA.2014.6907562.
29. Wirekoh J, Park Y-L. Design of flat pneumatic artificial muscles. *Smart Mater Struct* 2017;26:35009.
30. Niiyama R, *et al.* Pouch motors: printable soft actuators integrated with computational design. *Soft Robot* 2015;2: 59–70.
31. Niiyama R, Rognon C, Kuniyoshi Y. Printable pneumatic artificial muscles for anatomy-based humanoid robots. In: 2015 IEEE-RAS 15th International Conference on Humanoid Robots (Humanoids). IEEE, 2015, pp. 401–406. DOI: 10.1109/HUMANOIDS.2015.7363565.
32. Chang S-Y, *et al.* Design of small-size pouch motors for rat gait rehabilitation device. In: 2015 37th Annual International Conference of the IEEE Engineering in Medicine and Biology Society (EMBC) 2015. IEEE, 2015, pp. 4578–4581.
33. Yap HK, Sebastian F, Wiedeman C, Yeow C-H. Design and characterization of low-cost fabric-based flat pneumatic actuators for soft assistive glove application. In: 2017 International Conference on Rehabilitation Robotics (ICORR). IEEE, 2017, pp. 1465–1470. DOI:10.1109/ICORR.2017.8009454.
34. Sung C, Rus D. Foldable joints for foldable robots. *J Mech Robot* 2015;7:21012.
35. Klein R. Wiley InterScience (Online service). Laser welding of plastics. Wiley-VCH, Heidelberg, Germany, 2012.
36. Mutzenich S, Vinay T, Sood DK, Rosengarten G. Design parameter characterisation and experimental validation of hydrostatic actuation suitable for MEMS. *Sens Actuat A Phys* 2006;127:147–154.
37. Pak NN, III, RJW, Menciassi A, Dario P. Electrolytic silicone bourdon tube microactuator for reconfigurable surgical robots. In: Proceedings 2007 IEEE International Conference on Robotics and Automation. IEEE, 2007, pp. 3371–3376. DOI:10.1109/ROBOT.2007.363993.
38. Fan JA, *et al.* Fractal design concepts for stretchable electronics. *Nat Commun* 2014;5:ncomms4266.
39. Jang K-I, *et al.* Soft network composite materials with deterministic and bio-inspired designs. *Nat Commun* 2015;6:6566.

Address correspondence to:

*Bobak Mosadegh*  
*Department of Radiology*  
*Weill Cornell Medicine*  
*525 East 68th Street*  
*New York, NY 10021*

*E-mail:* bom2008@med.cornell.edu

*Simon Dunham*  
*Department of Radiology*  
*Weill Cornell Medicine*  
*525 East 68th Street*  
*New York, NY 10021*

*E-mail:* sid2012@med.cornell.edu